JOURNAL OF Materials CHEMISTRY

Molecular Lego®: non-centrosymmetric alignment within interdigitating layers

Geoffrey J. Ashwell,*[a] Richard Hamilton,[a] Barry J. Wood,[b] Ian R. Gentle[b] and Dejian Zhou[a]

[a]*The Nanomaterials Group, Centre for Photonics and Optical Engineering, The Whittle Building, Cranfield University, Cranfield, UK MK43 0AL. E-mail: g.j.ashwell@cranfield.ac.uk*
[b]*Department of Chemistry, University of Queensland, Brisbane, Australia QLD 4067*

Received 27th June 2001, Accepted 18th September 2001
First published as an Advance Article on the web 31st October 2001

(*E*)-*N*-Hexadecyl-4-[2-(4-octadecyloxynaphthyl)ethenyl]quinolinium bromide, which has a wide-bodied chromophore and terminal *n*-alkyl groups, adopts a U-shape when spread at the air–water interface but a stretched conformation when compressed to *ca.* 35 mN m^{-1}. The high-pressure phase has a narrow stability range prior to collapse but may be extended from 40 to 60 mN m^{-1} by co-spreading the dye in a 1 : 1 ratio with docosanoic acid. The mixed Langmuir–Blodgett (LB) film has a monolayer thickness of 4.6 ± 0.2 nm which decreases to 2.5 ± 0.1 nm layer^{-1} in the bulk, the reduction arising from an interdigitating layer arrangement, both top and bottom. It is the first example of LB-Lego® and, in addition, represents the only fully interdigitating structure with non-centrosymmetrically aligned chromophores. They are tilted 38° from the substrate normal. The second-harmonic intensity increases quadratically with the number of layers, *i.e.* as $I^{2\omega}{}_{(N)} = I^{2\omega}{}_{(1)} N^2$, with a second-order susceptibility of $\chi^{(2)}{}_{zzz} = 30$ pm V^{-1} at 1064 nm for refractive indices of $n^{\omega} = 1.55$ and $n^{2\omega} = 1.73$, $d = 2.5$ nm layer^{-1} and $\phi = 38°$. Angle resolved X-ray photoelectron spectra (XPS) of these films provide no evidence of the bromide counterion, which suggests that it is replaced by OH^- or HCO_3^-, which occur naturally in the aqueous subphase, or $C_{21}H_{43}COO^-$ from the co-deposited fatty acid. This probably applies to all cationic dyes deposited by the LB technique.

Introduction

Amphiphilic molecules spontaneously align at the air–water interface but tend to adopt a centric arrangement in the deposited film with the LB layers packing hydrophilically and hydrophobically at successive interfaces.[1–3] Thus, for applications where inversion symmetry is prohibited,[4] the layers should be interleaved with inactive spacers[5–12] or complementary dyes:[13–17] *e.g.* C_nH_{2n+1}–D–π–A and D–π–A–C_nH_{2n+1}, where the attachment of the hydrophobic tail is reversed relative to the donor–(π-bridge)–acceptor unit. But this results in the molecular dipole (D→A) being opposed to the interlayer dipole (A←D) and, therefore, it is also necessary to sterically hinder the interface to suppress charge-transfer.[17] Consequently, the chromophore is restricted to *ca.* 30% of the volume and to *ca.* 20% in films where the spacer is inactive. Improved occupancies are realised from molecules that align non-centrosymmetrically without the aid of spacers. It is necessary to suppress the head-to-head and tail-to-tail arrangements of conventional dyes and this is readily achieved when opposite ends of the D–π–A chromophore are substituted with *n*-alkyl groups.[18–21] The upper and lower surfaces of the LB layer will be hydrophobic if the molecules adopt a stretched rather than a U-shaped conformation and thus, if deposited only on the upstroke, the initial alignment at the air–water interface will be retained throughout the multilayer film.[3]

Progress in the design of materials for second-harmonic generation (SHG) necessitates an effective dilution of the active component if molecular organisation is realised by either electric field poling or LB deposition. When aligned in a polymer matrix, the volume of the optically nonlinear chromophore is limited to *ca.* 15% to avoid phase separation in poled films. This may be compared with *ca.* 20–30% in alternate-layer LB structures[5–17] and *ca.* 25–40% in the homomolecular LB films referred to above.[18–21] In this work, the volume of the chromophore layer has been increased to *ca.* 50% by using a wide-bodied chromophore with terminal *n*-alkyl groups. A favourable packing arrangement permits interdigitation both top and bottom, and has resulted in the first example of non-centrosymmetric Lego®. Consequently, the films show an improved second-order susceptibility.

Experimental

1-Octadecyloxy-4-naphthaldehyde

To an anhydrous solution of 1-octadecyloxynaphthalene (4.8 g, 12 mmol), previously obtained from the reaction of 1-naphthol, sodium hydroxide and 1-iodooctadecane, in DMF (30 cm^3) was added trichlorophosphine oxide (1.8 g, 24 mmol). The reaction mixture was stirred at room temperature for 1 h, then at 50 °C for 2 days, quenched by iced water (40 cm^3) and neutralised by aqueous sodium hydroxide. The resultant precipitate was purified by column chromatography on silica gel, eluting with 40–60 °C petroleum spirit–chloroform (3 : 1, v/v) to give a white microcrystalline solid: yield 2.0 g; 40%; mp 80–83 °C. δ_H (250 MHz, $CDCl_3$, *J*/Hz): 0.89 (t, *J* 6, 3H, CH_3), 1.28 (br s, 30H, CH_2), 1.92–2.02 (m, 2H, CH_2), 4.23 (t, *J* 6, 2H, CH_2O), 6.90 (d, *J* 6, 1H, Ar-H), 7.58 (t, *J* 8, 1H, Ar-H), 7.71 (t, *J* 8, 1H, Ar-H), 7.90 (d, *J* 8, 1H, Ar-H), 8.36 (d, *J* 8, 1H, Ar-H), 9.32 (d, *J* 8, 1H, Ar-H), 10.19 (s, 1H, CHO). *m*/*z* (FAB): 173 ($M^+ - C_{18}H_{36} + H$, 50%); 425 ($M^+ + H$, 100%).

(*E*)-*N*-Hexadecyl-4-[2-(4-octadecyloxynaphthyl)ethenyl]quinolinium bromide

To a solution of 1-octadecyloxy-4-naphthaldehyde (0.85 g, 2 mmol) and 1-hexadecyl-4-methylquinolinium bromide (0.90 g, 2 mmol) in methanol (30 cm^3) was added piperidine (0.4 cm^3) and the mixture heated under reflux for 10 h. Upon cooling, a

 DOI: 10.1039/b105657n

red microcrystalline product was filtered and then purified by column chromatography on silica gel, eluting initially with chloroform followed by chloroform–methanol (8 : 1, v/v): yield 1.0 g (60%); mp 200–202 °C (decomp.). λ_{max} ($CHCl_3$): 483 nm. δ_H (250 MHz, $CDCl_3$, *J*/Hz): 0.87 (t, *J* 6, 6H, CH_3), 1.26 (br s, 60H, CH_2), 1.80–1.99 (m, 4H, CH_2), 4.22 (t, *J* 6, 2H, CH_2O), 4.88 (t, *J* 6, 2H, CH_2N^+), 6.93 (d, *J* 8, 1H, Ar-H), 7.53 (t, *J* 7, 1H, Ar-H), 7.63 (t, *J* 8, 1H, Ar-H), 7.84–8.00 (m, 6H, Ar-H), 8.21 (t, *J* 8, 1H, Ar-H), 8.32 (d, *J* 8, 1H, Ar-H), 8.45–8.52 (m, 2H, Ar-H), 8.80 (d, *J* 8, 1H, Ar-H). *m/z* (FAB): 297 ($M^+-C_{34}H_{69}-Br^-$, 11%); 521 ($M^+-C_{18}H_{37}-Br^-$, 9%); 775 (M^++H-Br^-, 100%). Found, C, 76.9; H, 9.8; N, 1.4%. $C_{55}H_{84}NOBr$ requires: C, 77.25; H, 9.90; N, 1.64%.

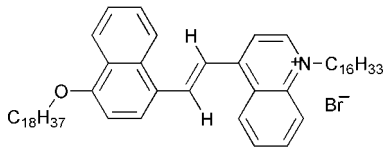

LB deposition

(*E*)-*N*-Hexadecyl-4-[2-(4-octadecyloxynaphthyl)ethenyl]quinolinium bromide was co-spread in a 1 : 1 ratio with docosanoic acid from chloroform onto the pure water subphase of an LB trough (Nima Technology, model 622), left for 10 min at 25 °C, and compressed at 0.5 $cm^2\ s^{-1}$, corresponding to a 0.1% s^{-1} change of the surface area. The mixed films were then deposited on the upstroke by passing the following substrates through the floating layer at a rate of 30 μm s^{-1} and a surface pressure of *ca.* 40 mN m^{-1}: silicon wafers for XPS studies (monolayer); gold-coated BK7 glass for surface plasmon resonance, SPR (1 to 25 layers), and hydrophilically treated glass slides for SHG (1 to 34 layers). The optical techniques have been previously described.[7,19]

XPS studies

LB films for angle resolved X-ray photoelectron spectroscopy (AR-XPS) studies were deposited onto silicon wafers. A Perkin-Elmer PHI model 560 spectrometer with a model 25–270 AR cylindrical mirror analyser and vacuum system, giving a base pressure of *ca.*10^{-9} Torr, was used for XPS measurements. Mg Kα X-rays (1253.6 eV) were generated from a magnesium anode operated at 15 kV and 400 W. Multiplex (narrow) scans, over selected elemental regions, were performed with a 50 eV pass energy at electron take-off angles of 87.7, 69.9, 51.5 and 34.5°. Quantitative analysis of the elements was based on the areas under peaks, fitted using a Gaussian–Lorentzian function with subtraction of a linear background. The values were corrected with atomic sensitivity factors as previously described.[22]

The elemental data and associated standard deviations, derived from the peak-fitting program, were analysed by fitting to a simple integral concentration depth-profile using a Monte-Carlo simulated annealing algorithm.[23] The electron mean free path for each element travelling through other elements was calculated by the method of Ashley.[24] The data were normalised by dividing by the intensity of the silicon substrate for each of the take-off angles. The substrate and film were then modelled as a semi-infinite silicon wafer, a silicon dioxide overlay and a partitioned organic layer. The probability of an electron, emitted in a lower layer, escaping through the subsequent upper layers was calculated for each of the atoms using exponential decay equations of the form given by Marshbanks *et al.*[25] The silicon and silicon dioxide intensities were initially fixed, using a simplex fit requiring adjustment of the thickness of the latter. The organic monolayer was then partitioned into many equidistant layers with groups of atoms (C, H, N and O) randomly distributed throughout the levels for theoretical analysis. Under the conditions set by the simulated annealing algorithm,[23] the atoms are randomly moved between layers; if the move improves the fit to the measured data, it is immediately accepted but, if not, the move is given the Metropolis[26] test which assigns an acceptance probability to the move. This procedure allows the algorithm to escape from local minima and improves the probability of finding the best configuration to fit the supplied data.

The result of the fit is such that the atoms align themselves in a configuration that resembles the distribution of the molecular structure. The number of levels occupied and average density of each level can then be used to calculate the implied thickness of the monolayer as well as the relative atomic positions.

Results and discussion

The pressure–area isotherm of the 1 : 1 mixed film of the dye and docosanoic acid exhibits three distinct regions: (i) a low-pressure regime with a limiting area of *ca.* 2.0 nm^2 $molecule^{-1}$, consistent with the two-legged molecule adopting a U-shaped conformation and aligning with its chromophore adjacent to the subphase; (ii) a broad transition at *ca.* 40 mN m^{-1}; (iii) a high-pressure regime with an area of 0.4 nm^2 $molecule^{-1}$ at the transition pressure (Fig. 1). The transition probably corresponds to a change in the conformation, from U-shaped to stretched, with the area being only slightly greater than the cross-section of the wide-bodied dye. Furthermore, when cycled between $0 \leqslant \pi \leqslant 50$ mN m^{-1}, the area is permanently reduced indicating that the molecule retains a stretched conformation. The concept may be controversial, as it requires one of the two hydrophobic groups to be adjacent to the aqueous subphase. However, the alternative explanation of multilayer formation, which could explain the reduced area, is dismissed because the monolayer thickness is reproducible and compatible with the molecular length. Thus, it may be assumed that repulsion between the hydrophobic tail and the subphase is offset by improved van der Waals tail-to-tail interactions in the condensed film. In addition, previous studies on related two-legged dyes have provided supporting evidence of a stretched conformation, the molecular areas in the high-pressure regimes being consistent with the isotherm data

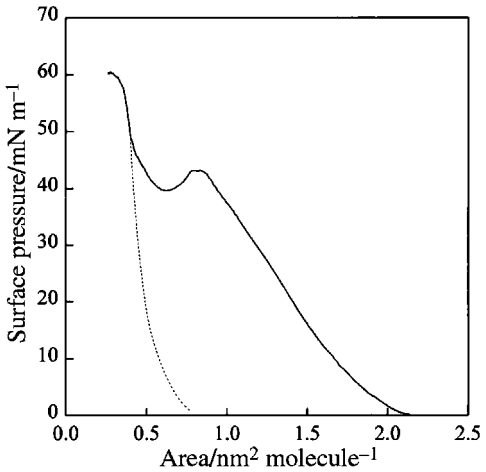

Fig. 1 Surface pressure *versus* area isotherm of a 1 : 1 mixed film of the dye and docosanoic acid showing a structural transition at *ca.* 40 mN m^{-1} and collapse at 60 mN m^{-1}. The area per molecule is permanently reduced when compressed above 40 mN m^{-1} (broken line) and this corresponds to a transition from a U-shaped to a stretched conformation. The pure dye has a similar isotherm but the high-pressure regime has a limited range with onset at 35 mN m^{-1} and collapse at 45 mN m^{-1}.

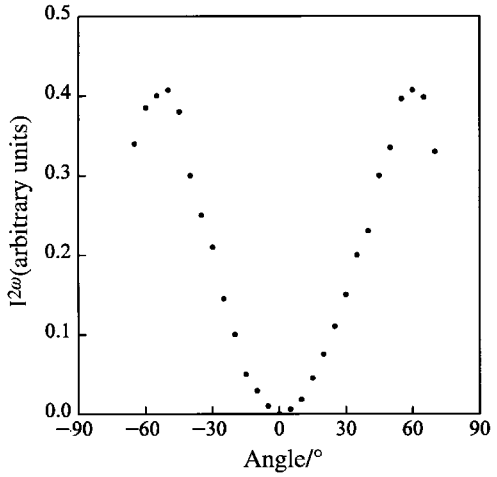

Fig. 2 Variation of the second-harmonic intensity with the angle of incidence of the laser beam (Nd : YAG, $\lambda = 1064$ nm, p polarised). The corresponding intensity for an s-polarised fundamental beam is greatly reduced and for clarity is not shown.

obtained here and confirmed by grazing incidence X-ray diffraction.[27]

Evidence that the transition does not correspond to a collapsed film is also indicated by the second-harmonic intensity which increases quadratically with the number of LB layers, *i.e.* as $I^{2\omega}{}_{(N)} = I^{2\omega}{}_{(1)}N^2$. The SHG data confirm non-centrosymmetric alignment and long-range structural order, which would not be expected for a collapsed film. A negligible second-harmonic intensity, when the laser beam is normal to the film (Fig. 2), confirms that the chromophore is tilted upwards and, using the method of Kajikawa *et al.*,[28] the polarisation dependence, $I^{2\omega}(\text{p}\rightarrow\text{p})/I^{2\omega}(\text{s}\rightarrow\text{p}) = 10$ at 45°, corresponds to a tilt angle of 38° from the vertical. This is also indicative of a stretched rather than a U-shaped conformation as the latter would be expected to align the chromophores parallel to the substrate with both hydrophobic groups pointing either up or down.

The XPS data from monolayer films on silicon wafers show unexpected behaviour in so far as the bromide, which has a high atomic sensitivity factor, is not observed. This may be explained by anion exchange because, when on an aqueous subphase prior to deposition, the water-soluble counterion dissolves leaving the cationic dye and docosanoic acid at the air–water interface. The resultant bromide concentration in the subphase of the LB trough is typically *ca.* 5×10^{-8} mol dm^{-3} and significantly less than those of OH^- and HCO_3^-, which occur naturally. Thus, it may be assumed that either of these or the docosanoate act as the counterion. Quantitative analysis of the angle-resolved XPS data for C, N and O (Fig. 3) has provided a monolayer thickness of 4.7 ± 0.7 nm as well as the depth profile of each of the elements. Consistent with the explanation above, *i.e.* a stretched molecular conformation, the hydrophobic alkyl tails are top and bottom with narrow bands of nitrogen and oxygen, *ca.* 0.5 ± 0.1 nm thick, located close to the middle of the film: the nitrogen layer is centred 2.1 ± 0.2 nm from the substrate and the oxygen layer at 2.6 ± 0.2 nm. The

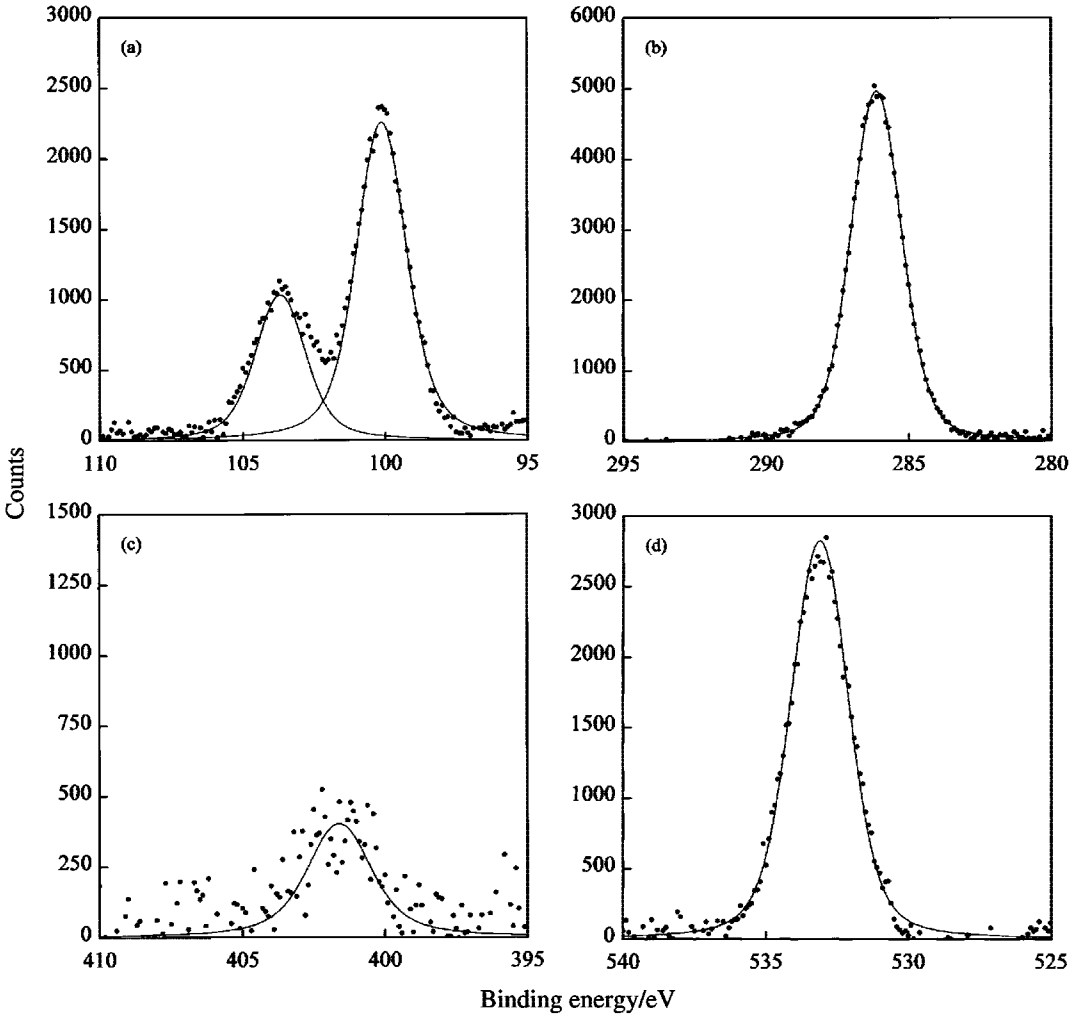

Fig. 3 XPS spectra of an LB monolayer of the mixed film on a silicon wafer with an electron take-off angle of 87.7°: (a) silicon where the weaker peak corresponds to SiO_2; (b) carbon; (c) nitrogen and (d) oxygen.

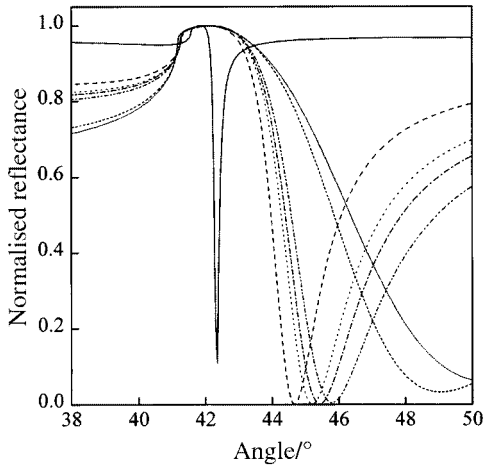

Fig. 4 Normalised reflectance *vs.* the angle of incidence for a glass/Au/monolayer structure of the mixed LB film at 1064 nm (Nd : YAG laser), 632.8, 611.9, 604.0, 594.1 and 543.5 nm (HeNe) and 532 nm (frequency doubled Nd : YAG). The resonant angle increases with decreasing wavelength. The 250 data points per curve have been omitted but the theoretical fits directly overlap the experimental results.

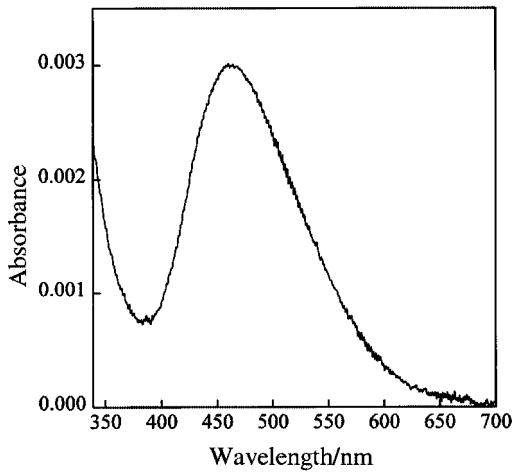

Fig. 5 UV/visible spectrum of an LB multilayer of the mixed film, the absorbance being normalised to that of the monolayer.

thickness of the amorphous silicon dioxide layer is 1.8 nm assuming a density of 2.3 Mg m^{-3}.

The monolayer thickness from the XPS data above is consistent with values derived from the surface plasmon resonance (SPR) data from glass/Au/monolayer structures (Fig. 4), studied by attenuated total reflection in the Kretschmann configuration.[29] Analysis of the data gave a mean thickness of 4.6 ± 0.2 nm with refractive indices as follows: $n = 1.55$ at 1064 nm (infrared); 1.59 at 632.8 nm (red); 1.62 at 611.9 nm (red); 1.63 at 604.0 nm (orange); 1.64 at 594.1 nm (yellow); 1.66 at 543.5 nm (green); 1.73 at 532.0 nm (green) with standard deviations of ± 0.03. The progressive increase of the index with decreasing wavelength is consistent with the absorption characteristics of the film (Fig. 5), there being a broad peak with $\lambda_{max} = 460$ nm and cut-off above *ca.* 700 nm.

The multilayer films have two structural forms. The molecular layers of phase I pack conventionally with a mean spacing of 4.3 ± 0.3 nm $layer^{-1}$ in the bulk film, the data being obtained by analysis of the SPR spectra (Fig. 6). This is consistent with the molecular length of 5.3 nm when a tilt of 38°, from the SHG polarisation dependence, is taken into account. In contrast, a reduced layer spacing of only 2.5 ± 0.2 nm $layer^{-1}$ for phase II (Fig. 7) suggests a Lego® arrangement, with interdigitation both top and bottom. This may be anticipated by the fact that the wide-bodied chromophore has a cross-sectional area of *ca.* 0.4 nm^2 compared with 0.2 nm^2 for each of its hydrophobic tails. There is sufficient space and, thus, it is assumed that an open surface structure would facilitate interdigitation.

In such films the role of the docosanoic acid, co-deposited in a 1 : 1 ratio with the wide-bodied dye, is unclear but it stabilises the floating monolayer in the high-pressure region of the isotherm. It is unknown whether phase separation occurs or, as indicated by the XPS data, whether the docosanoate anion replaces the bromide counterion in the deposited film. However, regardless of these uncertainties, the films exhibit a quadratic dependence of the second-harmonic intensity with the number of layers and have a second-order susceptibility of $\chi^{(2)}_{zzz} = 30$ pm V^{-1} at 1064 nm for $l = 2.5$ nm $layer^{-1}$, $\phi = 38°$, $n^{\omega} = 1.55$ and $n^{2\omega} = 1.73$. The value obtained for the non-interdigitating structure is lower because, for the same intensity, the susceptibility is proportional to the reciprocal of the thickness. Thus, an important feature of the interdigitating layers concerns the effective thickness of the

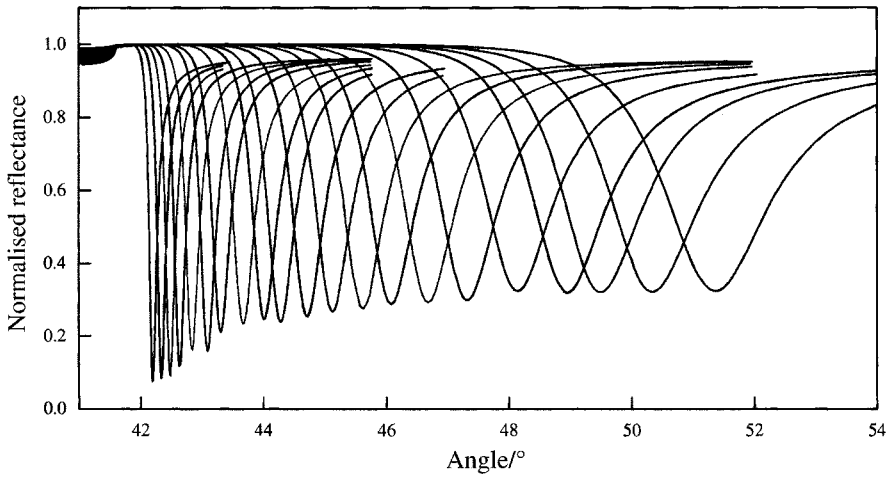

Fig. 6 Normalised reflectance *vs.* the angle of incidence for glass/Au and glass/Au/LB structures comprising from one to twenty non-interdigitating LB layers of the mixed film at $\lambda = 1064$ nm. The SPR spectra broaden with thickness and for clarity the data for twenty-five LB layers has been omitted. The thickness and dielectric permittivities of the gold overlay are $l = 47.5 \pm 0.3$ nm, $\varepsilon_r = -47.4 \pm 0.4$ and $\varepsilon_i = 3.1 \pm 0.3$. Corresponding values for the LB overlay are 4.3 ± 0.3 nm $layer^{-1}$ with $\varepsilon_r = 2.4 \pm 0.1$ and $\varepsilon_i = 0$, the data being independent of the number of deposited layers. The 250 data points per curve have been omitted but the theoretical fits directly overlap the experimental results.

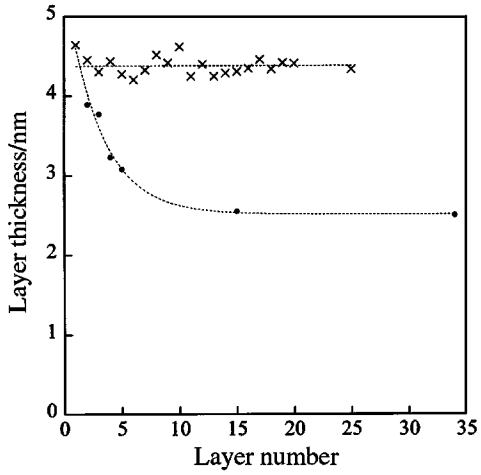

Fig. 7 Layer thickness *vs.* the layer number in conventional (×, phase I) and interdigitating (●, phase II) LB films by analysis of the SPR spectra, the data for two to five layers relating to the increase in thickness and thereafter to the mean. The corresponding thickness for 34 layers is from ref. 27.

hydrophobic alkyl groups, which is *ca.* 50% of the film compared with *ca.* 80% of the molecular length.

Conclusion

The two-legged dye molecule adopts a stretched rather than a U-conformation when deposited from the high-pressure region of the isotherm. This is confirmed by the monolayer thickness, 4.6 ± 0.2 nm by analysis of the SPR data (*cf.* 4.7 ± 0.7 nm from XPS), the depth profile of the constituent elements from the angle resolved XPS data, and a chromophore tilt angle of 38° from the polarisation dependence of the second-harmonic intensity. Furthermore, the bulk film has two structural forms in which the layers either pack conventionally (phase I: 4.3 ± 0.3 nm layer^{-1}) or interdigitate (phase II: 2.5 ± 0.2 nm layer^{-1}). The latter is the first example of LB-Lego® although examples of molecular zips, which interdigitate at a single interface, are also known.[5,6] It is also the only example to date of a fully interdigitating structure where the optically nonlinear chromophores are non-centrosymmetrically aligned.

Preliminary accounts of this work were presented at the International Conference of Organic Molecular Electronics for the Twenty-first Century (Nagoya)[30] and the International Conference of Synthetic Metals (Bad Gastein).[31] These focussed upon a quadratic increase of the second-harmonic intensity with the number of layers and the thickness of a 34 layer film. Such results are excluded from this publication and the extended investigation primarily relates to film characterisation by angle resolved XPS and SPR studies.

Acknowledgements

One of us (G.J.A.) is grateful to the Engineering and Physical Sciences Research Council (UK) for support of this work and for providing a studentship (to R.H.). We also acknowledge Nick Calos for assistance with the methodology of analysis of the angle resolved XPS data.

References

1 A. Ulmann, *An Introduction to Ultrathin Films: from Langmuir–Blodgett to Self-Assembly*, Academic Press, San Diego, 1991.
2 M. C. Petty, *Langmuir–Blodgett Films: an Introduction*, Cambridge University Press, Cambridge, 1996.
3 G. J. Ashwell, *J. Mater. Chem.*, 1999, **9**, 1991.
4 C. Bosshard, K. Sutter, P. Prêtre, J. Hulliger, M. Flörsheimer, P. Kaatz and P. Günter, *Organic Nonlinear Optical Materials, Advances in Optics*, Vol. 1, ed. A. F. Garito and F. Kajzar, Gordon and Breach, Basel, 1995.
5 G. J. Ashwell, E. J. C. Dawnay, A. P. Kuczynski and P. J. Martin, *Proc. SPIE–Int. Soc. Opt. Eng.*, 1991, **1361**, 589.
6 S. H. Ma, X. Z. Lu, J. H. Xu, W. C. Wang and Z. M. Zhang, *J. Phys. D*, 1997, **30**, 2651.
7 G. J. Ashwell, P. D. Jackson, D. Lochun, P. A. Thompson, W. A. Crossland, G. S. Bahra, C. R. Brown and C. Jasper, *Proc. R. Soc. London A*, 1994, **455**, 385.
8 P. Hodge, Z. Ali-Adib, D. West and T. A. King, *Macromolecules*, 1993, **26**, 1789.
9 G. Wang, J. Wen, X. Lu, L. Liu, W. Wang, Y. Huang, H. Al, Y. Fang and F. Tao, *J. Phys. D*, 1995, **28**, 2113.
10 M. Era, K. Nakamura, T. Tsutsui, S. Saito, H. Niino, K. Takehara, K. Isomura and H. Tanaguchi, *Jpn. J. Appl. Phys.*, 1992, **210-211**, 163.
11 I. Cabrera, A. Mayer, D. Lupo, U. Falk, U. Scheunemann and W. Hickel, *Nonlinear Opt.*, 1995, **9**, 161.
12 G. J. Ashwell, A. J. Whittam, M. A. Amiri, R. Hamilton, A. Green and U.-W. Grummt, *J. Mater. Chem.*, 2001, **11**, 1345.
13 M. J. Roberts, G. A. Lindsay, K. J. Wynne, R. A. Hollins, P. Zarras, J. D. Stenger-Smith, M. Nadler and A. P. Chafin, *Polym. Prepr. (Am. Chem. Soc., Div. Polym. Chem.)*, 1997, **38**, 975.
14 H. R. Motschmann, T. L. Penner, N. J. Armstrong and M. C. Ezenyilimba, *J. Phys. Chem.*, 1993, **97**, 3933.
15 W. M. K. P. Wijekoon, S. K. Wijaya, J. D. Bhawalkar, P. N. Prasad, T. L. Penner, N. J. Armstrong, M. C. Ezenyilimba and D. J. Williams, *J. Am. Chem. Soc.*, 1996, **118**, 4480.
16 (*a*) G. A. Lindsay, K. J. Wynne, W. N. Herman, A. P. Chafin, R. A. Hollins, J. D. Stenger-Smith, J. Hoover, J. Cline and M. J. Roberts, *Nonlinear Opt.*, 1996, **15**, 139; (*b*) G. A. Lindsay, M. J. Roberts, J. D. Stenger-Smith, W. N. Herman, P. R. Ashley and K. J. Wynne, *Naval Res. Rev.*, 1997, **XLIX**, 21.
17 G. J. Ashwell, D. Zhou, K. Skjonnemand and R. Ranjan, *Aust. J. Chem.*, 2001, **54**, 19.
18 G. J. Ashwell, P. D. Jackson and W. A. Crossland, *Nature*, 1994, **368**, 438.
19 (*a*) G. J. Ashwell, G. Jefferies, C. D. George, R. Ranjan, R. B. Charters and R. P. Tatam, *J. Mater. Chem.*, 1996, **6**, 131; (*b*) G. J. Ashwell, G. Jefferies and R. Ranjan, *Electron. Lett.*, 1996, **32**, 59.
20 G. J. Ashwell, T. Handa and R. Ranjan, *J. Opt. Soc. Am. B.*, 1998, **15**, 466.
21 (*a*) G. J. Ashwell, R. Ranjan, A. J. Whittam and D. S. Gandolfo, *J. Mater. Chem.*, 2000, **10**, 63; (*b*) G. J. Ashwell and D. S. Gandolfo, *J. Mater. Chem.*, 2001, **11**, 246.
22 R. J. Ward and B. J. Wood, *Surf. Interf. Anal.*, 1992, **18**, 679.
23 S. Kirkpatrick, C. D. Gelatt and M. P. Vecchi, *Science*, 1983, **220**, 671.
24 J. C. Ashley, *IEEE Trans. Nucl. Sci.*, 1980, **27**, 1454.
25 T. L. Marshbanks, H. K. Jugduth, W. N. Delgass and E. I. Franses, *Thin Solid Films*, 1993, **232**, 126.
26 N. Metropolis, A. Rosenbluth, M. Rosenbluth, A. Teller and E. Teller, *J. Chem. Phys.*, 1953, **21**, 1087.
27 G. J. Ashwell, P. D. Jackson, G. Jefferies, I. R. Gentle and C. H. L. Kennard, *J. Mater. Chem.*, 1996, **6**, 137.
28 K. Kajikawa, K. Kigata, H. Takezoe and A. Fukuda, *Mol. Cryst. Liq. Cryst.*, 1990, **182**, 91.
29 E. Kretschmann, *Z. Phys.*, 1971, **241**, 313.
30 G. J. Ashwell, D. Zhou and K. Skjonnemand, *IEICE Trans*, 2000, **E83-C**, 1057.
31 G. J. Ashwell, D. Zhou, R. Hamilton, K. Skjonnemand and A. Green, *Synth. Met.*, 2001, **121**, 1455.